JCB Article

A transgene carrying an A2G missense mutation in the SMN gene modulates phenotypic severity in mice with severe (type I) spinal muscular atrophy

Umrao R. Monani,[1] Matthew T. Pastore,[2] Tatiana O. Gavrilina,[1] Sibylle Jablonka,[5] Thanh T. Le,[2] Catia Andreassi,[1] Jennifer M. DiCocco,[2] Christian Lorson,[6] Elliot J. Androphy,[7] Michael Sendtner,[5] Michael Podell,[3] and Arthur H.M. Burghes[1,2,4]

[1]Departments of Neurology, [2]Molecular and Cellular Biochemistry, [3]Veterinary Clinical Sciences, and [4]Molecular Genetics, Ohio State University, Columbus, OH 43210
[5]Institute of Clinical Neurobiology, University of Würzburg, D-97080 Würzburg, Germany
[6]Department of Biology, Arizona State University, Tempe, AZ 85287
[7]Department of Medicine, University of Massachusetts Medical School, Worcester, MA 01605

5q spinal muscular atrophy (SMA) is a common autosomal recessive disorder in humans and the leading genetic cause of infantile death. Patients lack a functional survival of motor neurons (*SMN1*) gene, but carry one or more copies of the highly homologous *SMN2* gene. A homozygous knockout of the single murine *Smn* gene is embryonic lethal. Here we report that in the absence of the *SMN2* gene, a mutant SMN A2G transgene is unable to rescue the embryonic lethality. In its presence, the A2G transgene delays the onset of motor neuron loss, resulting in mice with mild SMA. We suggest that only in the presence of low levels of full-length SMN is the A2G transgene able to form partially functional higher order SMN complexes essential for its functions. Mild SMA mice exhibit motor neuron degeneration, muscle atrophy, and abnormal EMGs. Animals homozygous for the mutant transgene are less severely affected than heterozygotes. This demonstrates the importance of SMN levels in SMA even if the protein is expressed from a mutant allele. Our mild SMA mice will be useful in (a) determining the effect of missense mutations in vivo and in motor neurons and (b) testing potential therapies in SMA.

Introduction

Proximal spinal muscular atrophy (SMA)* is a common autosomal recessive neurodegenerative disease in humans characterized by loss of the spinal motor neurons and atrophy of the limb and trunk muscles (Crawford and Pardo, 1996; Melki, 1997). It occurs with a frequency of 1 in 10,000 individuals and is the most common genetic cause of infant mortality (Roberts et al., 1970). Based on the age at onset and severity of the disease phenotype, the proximal SMAs have been classified into type I (severe), type II (intermediate), and type III (mild) SMA (Munsat and Davies, 1992). All three forms of the disease are due to loss or mutation of the telomeric survival of motor neurons gene (*SMN1*) (Bussaglia et al., 1995; Lefebvre et al., 1995; Parsons et al., 1996; Hahnen et al., 1997; Talbot et al., 1997). Mutations in an almost identical copy gene, *SMN2*, do not cause disease. The critical difference between the two genes is a C to T transition in exon 7 of *SMN2*, which affects splicing of this exon (Lorson et al., 1999; Monani et al., 1999a). Thus, *SMN1* produces a majority of the full-length SMN transcript, whereas *SMN2* generates mostly an isoform lacking exon 7. The protein product of the Δ7 transcript is thought to be unstable and rapidly degraded (Lorson and Androphy, 2000). SMA patients who lack *SMN1* but carry a varying number of copies of *SMN2* presumably produce insufficient full-length SMN protein for motor neuron survival. The disease phenotype is

The online version of this article includes supplemental material.

U.R. Monani and M.T. Pastore contributed equally to this work.

Address correspondence to Umrao R. Monani, Department of Molecular and Cellular Biochemistry, 363 Hamilton Hall, 1645 Neil Avenue, Columbus, OH 43210. Tel.: (614) 688-4759. Fax: (614) 292-4118. E-mail: monani.2@osu.edu; or Arthur H.M. Burghes, Department of Molecular and Cellular Biochemistry, 363 Hamilton Hall, 1645 Neil Avenue, Columbus, OH 43210. Tel.: (614) 688-4759. Fax: (614) 292-4118. E-mail: burghes.1@osu.edu

*Abbreviations used in this paper: EMG, electromyograph; MNCV, motor nerve conduction velocity; MUNE, motor unit number estimation; SMA, spinal muscular atrophy; SMN, survival of motor neurons.

Key words: SMA; SMN; mouse model; motor neurons; transgene

The Journal of Cell Biology, Volume 160, Number 1, January 6, 2003 41–52
http://www.jcb.org/cgi/doi/10.1083/jcb.200208079

The Journal of Cell Biology

modulated by *SMN2* copy number, likely due to the low levels of full-length SMN produced by *SMN2* (Campbell et al., 1997; McAndrew et al., 1997).

The 38-kD SMN protein is ubiquitously expressed (Coovert et al., 1997; Lefebvre et al., 1997), often localizing in dot-like structures termed gems. Gems overlap with, or are in close proximity to, coiled bodies (Liu and Dreyfuss, 1996; Young et al., 2000). SMN is thought to be important in snRNP biogenesis and mRNA splicing (Pellizzoni et al., 1998), but is most likely a multifunctional molecule (Fischer et al., 1997; Liu et al., 1997; Buhler et al., 1999; Strasswimmer et al., 1999; Charroux et al., 1999; Campbell et al., 2000; Gangwani et al., 2001; Jones et al., 2001; Pellizzoni et al., 2001a,b; Terns and Terns, 2001; Young et al., 2001). However, it is not clear which of SMN's functions is critical specifically to motor neurons.

In keeping with its housekeeping functions, an *Smn* knockout in mice is embryonic lethal (Schrank et al., 1997). To create a viable animal model of SMA, the *SMN2* gene was introduced into $Smn^{-/-}$ mice (Hsieh-Li et al., 2000; Monani et al., 2000). One to two–copy $SMN2;Smn^{-/-}$ mice exhibit a type I SMA phenotype. 8–16 copies of *SMN2* completely ameliorate the disease phenotype. Inducing *SMN2* to produce higher levels of SMN protein therefore seems an attractive option in treating SMA. A number of groups have reported molecules capable of inducing *SMN2* to produce higher levels of SMN (Baron-Delage et al., 2000; Andreassi et al., 2001; Chang et al., 2001; Zhang et al., 2001). It is essential that these be tested in appropriate animal models before human clinical trials are undertaken. Although the existing animal models have been extremely important in furthering the understanding of the pathophysiology of the SMA disease process, it is clear that a more suitable animal model is needed to address the next generation of in vivo experiments. In this study, we show that an SMN A2G missense mutation rescues the severe SMA phenotype in low copy $SMN2;Smn^{-/-}$ mice but is unable to rescue $Smn^{-/-}$ embryonic lethality in the absence of the *SMN2* gene. Increased SMN protein in $SMN\ A2G;SMN2;Smn^{-/-}$ mice affects the timing of motor neuron loss and results in animals with a mild SMA phenotype. Mild SMA mice exhibit muscle atrophy, motor neuron degeneration, and abnormal electromyographs (EMGs). These characteristics, in particular the electrophysiology, serve as easily assayed outcome measures in therapeutic strategies in SMA. Importantly, we also show that SMN A2G is unable to efficiently self-associate, a property required for the formation of "active" SMN complexes. We suggest that mutant oligomers are unstable and fail to bind components that are essential for one or more of SMN's functions. This results in a rapid turnover of the protein, underlining the importance of some, albeit low levels of, full-length SMN in the SMN complex and provides insight into the mechanism involving functional complex formation.

Results

Generation of transgenic mice and genotype–phenotype analysis

We previously identified three unrelated SMA patients (two with type III SMA and one with type II SMA) carrying a single *SMN2* allele and an SMN A2G missense mutation (Parsons et al., 1998). A cDNA carrying the A2G mutation under a 3.4-kb SMN promoter fragment (Monani et al., 1999b) (Fig. 1 A) was microinjected into fertilized mouse oocytes. Of the four founders obtained, the two transmitting lines, 2002 and 2023, were first analyzed for transgene copy number and then mated to low copy $SMN2;Smn^{+/-}$ mice (Monani et al., 2000). To assess the number of copies of the SMN A2G allele in each of the lines, Southern blot analysis of tail DNA using probes that bound SMN A2G and murine *Smn*, respectively, was performed. Relative to the single copy murine *Smn* gene, line 2002 was found to have 15 copies of the transgene whereas line 2023 carried 11 copies (Fig. 1 B). Double transgenic $SMN\ A2G;SMN2;Smn^{+/-}$ mice were interbred or crossed to $SMN2;Smn^{+/-}$ animals, resulting in mice carrying one or two copies of *SMN2* and the mutant transgene but completely lacking mouse *Smn* ($SMN\ A2G;SMN2;Smn^{-/-}$) (Fig. 1 C). Mice of this genotype from line 2002 were no different from the severe type I SMA mice we have previously described. On Western blot analysis, this line was found not to express the A2G transgene (unpublished data), possibly due to a site-specific integration effect. However, $SMN2;Smn^{-/-}$ mice carrying the A2G transgene from line 2023 display all of the characteristics of type III SMA. $Smn^{-/-}$ animals with a single copy of *SMN2* and heterozygous for the A2G transgene are 20–40% smaller (1.14 ± 0.06; $n = 5$) than their normal littermates (1.62 ± 0.18; $n = 11$) at birth and continue to remain so during development and into adulthood (Fig. 1, D and F). At 3 wk of age, these mice are less active than normal sibs. In addition, they begin to display signs of muscle weakness, as evidenced by a tendency to clasp the hind limbs when suspended by the tail (Fig. 1 E). $SMN2;Smn^{-/-}$ mice that are homozygous for the A2G transgene have a considerably milder phenotype and are indistinguishable from normal littermates often into adulthood. This is consistent with previous reports indicating a tight correlation between *SMN2* copy number/protein levels and disease severity (Lefebvre et al., 1997; Coovert et al., 1997). Both heterozygous and homozygous A2G $SMN2;Smn^{-/-}$ mice breed, although the former are less efficient and live $\leq$1 yr. Mean survival of heterozygous A2G $SMN2;Smn^{-/-}$ mice is 227 d ($n = 14$) versus 5.16 d for type I SMA mice ($n = 57$) and 736 d for $Smn^{+/-}$ mice ($n = 12$) (see Fig. S1, available online at http://www.jcb.org/cgi/content/full/jcb.200208079/DC1). Toward the end of their lives, type III SMA mice heterozygous for the A2G transgene exhibit very little activity, short, shallow breathing, lose considerable weight, and fail to groom efficiently. In contrast, the oldest $SMN2;Smn^{-/-}$ mice homozygous for the A2G transgene are currently 15 mo of age, healthy, and the males continue to breed well.

To determine whether the mutant A2G transgene is capable of rescuing $Smn^{-/-}$ embryonic lethality on its own, $SMN\ A2G;Smn^{+/-}$ intercrosses were set up. Out of 102 progeny mice genotyped, none were found to be $Smn^{-/-}$. This suggests that the A2G mutant transgene is unable to rescue embryonic lethality. To determine when embryonic lethality occurs in $SMN\ A2G;Smn^{-/-}$ mice, E12 embryos ($n = 60$)

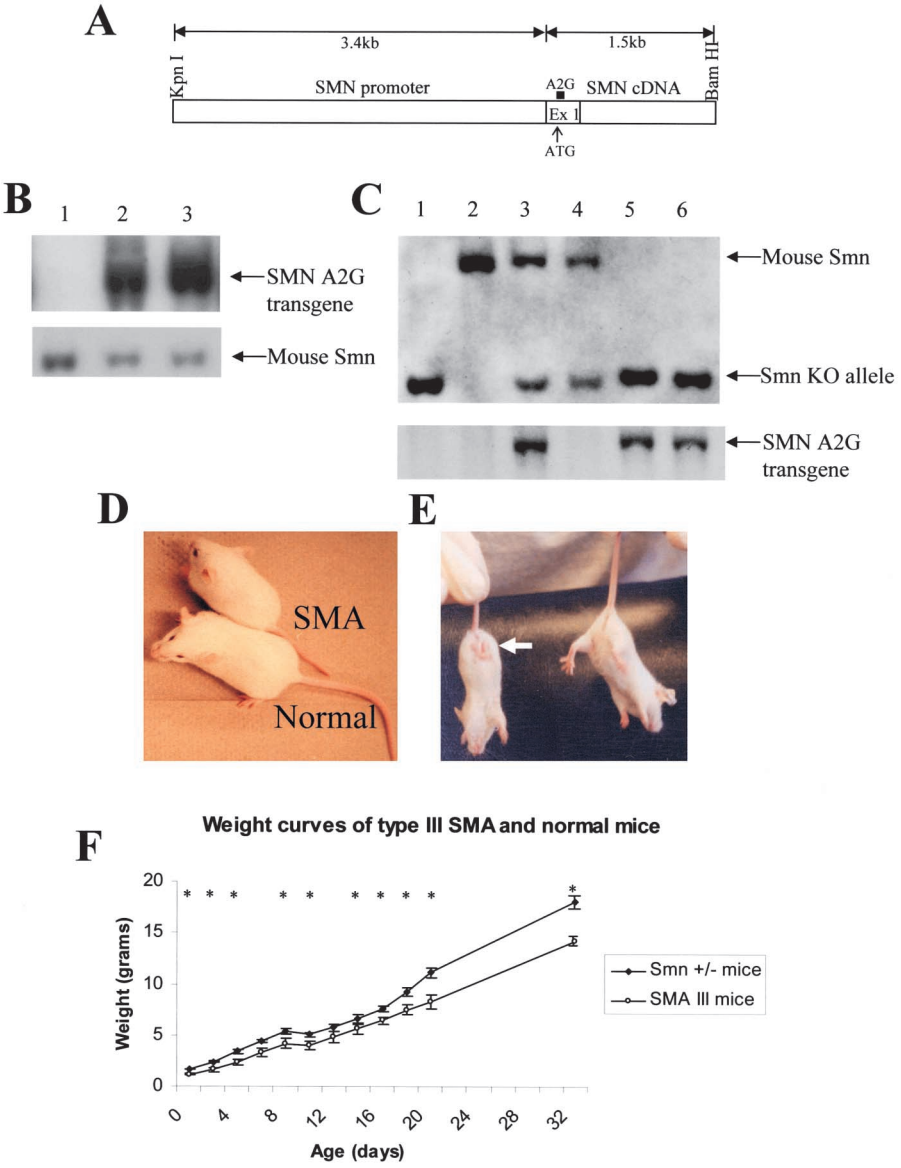

Figure 1. **Generation and characterization of mild SMA mice.** (A) Schematic representation of the 4.9-kb SMN A2G mutant transgene used to create transgenic mice. (B) Transgene copy number using Southern blot analysis. The blot was simultaneously probed with fragments that recognize the transgene and murine *Smn*, respectively. The latter, which is present in two copies per genome, serves as an internal control. Lane 1, DNA from a nontransgenic $Smn^{+/+}$ animal; lane 2, line 2023; lane 3, line 2002. (C) Southern blot analysis after BamHI digestion of tail DNA from mice from line 2023. Presence/absence of the wild-type murine *Smn* and *Smn* knockout (KO) allele was determined using a probe in murine *Smn* intron 1. Lane 1, type I SMA mouse control; lane 2, $Smn^{+/+}$ normal mouse; lane 3, *SMN A2G;SMN2;*$Smn^{+/-}$ female mouse; lane 4, *SMN2;*$Smn^{+/-}$ male lacking the A2G transgene; lanes 5 and 6, type III SMA pups of mice from lanes 3 and 4. Note that after genotyping for murine wild-type *Smn* and the KO alleles, the blot was stripped and reprobed to check for the presence of the A2G transgene. Genotyping for *SMN2* was done by PCR (not depicted). 1-mo-old type III SMA mouse and a normal littermate showing a difference in size (D) and muscle weakness (E), as displayed by a hindlimb clasping reflex (arrow) in the former. Four of four type III SMA animals heterozygous for the A2G transgene displayed this reflex, compared with one out of four type III SMA animals homozygous for the mutant transgene and one of five normal littermates. (F) Weight curves of mild SMA mice ($n = 5$) heterozygous for the A2G transgene and *SMN2* and normal littermates ($n = 5$). Error bars indicate standard deviation. An asterisk indicates that there was a significant difference ($P < 0.05$, *t* test) in weights measured on the given days. As adults (33 d of age), mild SMA mice were significantly smaller (14.16 ± 0.52 g; $n = 5$) than normal littermates (18.02 ± 1.08 g; $n = 5$).

from *SMN A2G;*$Smn^{+/-}$ intercrosses were genotyped. None were found to be $Smn^{-/-}$, indicating that death occurs before this stage in development. This is similar to $Smn^{-/-}$ and $Smn^{\delta7/\delta7}$ mice, which also die early in embryogenesis (Schrank et al., 1997; Hsieh-Li et al., 2000).

Decreased self-association of mutant A2G SMN molecules

SMN self-associates using domains encoded by exons 2b and 6 (Lorson et al., 1998; Young et al., 2001). We investigated the effect of the missense A2G mutation on self-association. A GST–SMN A2G fusion protein was immobilized on glutathione-linked agarose beads and then incubated with ^{35}S-labeled SMN A2G protein. Bound fractions were washed extensively and resolved by SDS-PAGE. As controls, similar self-association studies were performed with full-length SMN and Δ7 SMN. Our results show that SMN A2G molecules self-associate with an efficiency between that of full-length SMN and Δ7 SMN (Fig. 2 A) as do other mild SMA mutations (Lorson et al., 1998). This is consistent with the mild SMA phenotype we see in patients carrying this mutation and our *SMN A2G;SMN2;*$Smn^{-/-}$ mice. To determine the effect of the A2G mutation on the ability of the mutant protein to bind native full-length (FL) SMN and Sm proteins, GST–SMN and GST–SmN fusion proteins immobilized on agarose beads were incubated with labeled SMN A2G. Bound fractions were washed as described above. As a comparison, the ability of Δ7 SMN and FL-SMN each to bind to SmN and native SMN was assessed. As expected, SMN A2G binds FL-SMN with a higher affinity than does Δ7 SMN but with a lower affinity than does native SMN (Fig. 2 B). Interestingly, the ability of SMN A2G to bind the Sm protein SmN was greatly decreased even though the mutation does not lie in the Sm binding domain (Fig. 2 C).

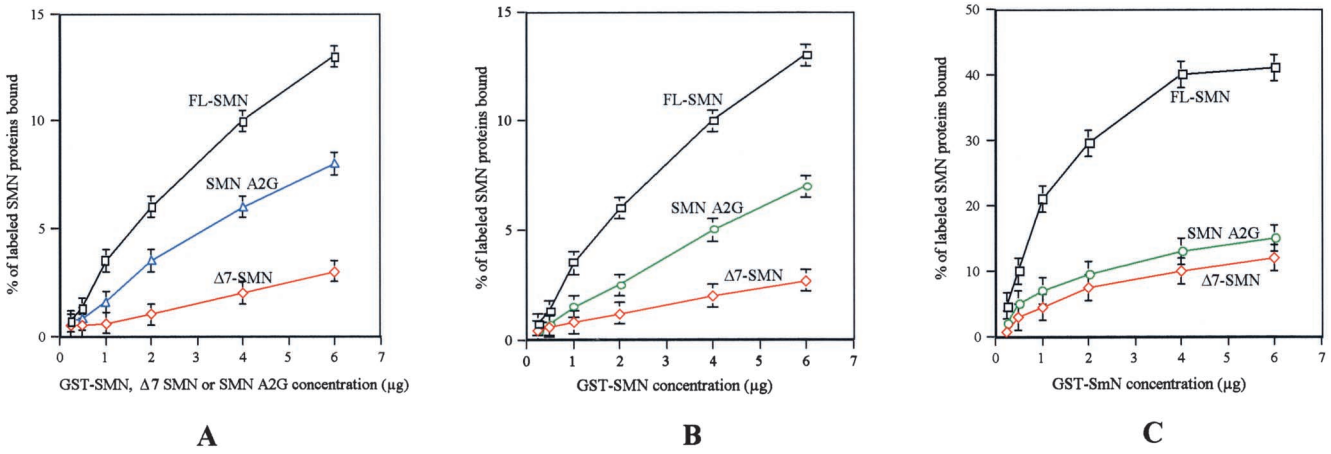

Figure 2. **In vitro binding studies on SMN A2G.** (A) Self-association studies between ^{35}S-labeled SMN proteins and bound GST–SMN fusion proteins. (B) The interaction of SMN A2G, FL-SMN, and Δ7 SMN each with FL-SMN. (C) Binding of FL-SMN, SMN A2G, or Δ7 SMN (as indicated) with the Sm protein SmN. In all three studies, binding values were calculated as a % of ^{35}S-labeled SMN A2G, FL-SMN, or Δ7 SMN.

Expression of the mutant SMN A2G transgene

To assess the expression of the SMN A2G transgene, RT-PCR studies (Fig. 3 A) on A2G animals lacking *SMN2* and Western blot analyses on mild SMA animals (Figs. 3, B and C) were performed. Our data show that the transgene is expressed in all of the tissues examined. This is similar to the expression of the endogenous gene, suggesting that the 3.4-kb promoter fragment used here contains the necessary elements for ubiquitous expression. Western blot analysis performed on *SMN A2G;SMN2;Smn*$^{-/-}$ animals shows that mild SMA mice express significantly higher SMN levels than do age-matched type I SMA mice, but not as much as normal littermates (Fig. 3 B). Furthermore, type III SMA animals homozygous for the A2G transgene express higher levels of the SMN protein than do heterozygous animals (Fig. 3 C). This is consistent with previous data showing that a tight correlation exists between SMN levels and phenotypic severity in SMA.

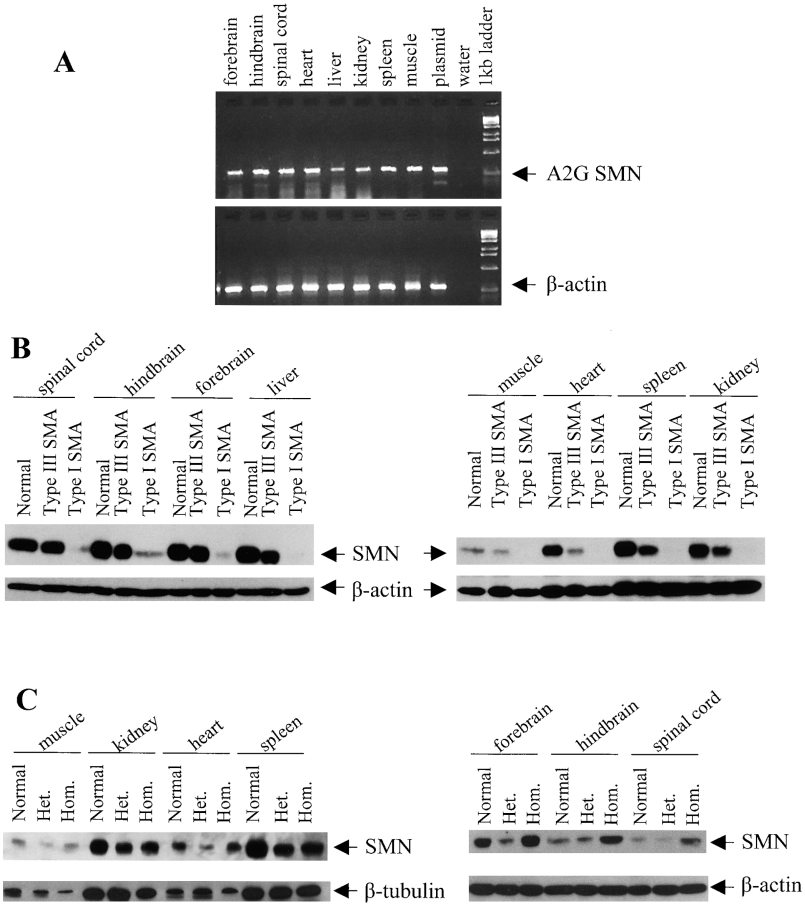

Figure 3. **Expression analysis of the mutant SMN A2G transgene in transgenic mice.** (A) RT-PCR on RNA from indicated tissues of an *SMN A2G;Smn*$^{+/+}$ animal was performed as described in the Materials and methods. The β-actin gene was simultaneously amplified as a control. (B) Western blot analysis on 5-d-old type I SMA, type III SMA, and an *Smn*$^{+/-}$ mouse was performed using the anti-SMN monoclonal antibody, MANSMA2. The blot was subsequently stripped and probed with an anti–β-actin antibody to control for loading amounts. Type I SMA mice produce very little SMN, which is visible only after longer exposures. (C) Western blot analysis on 3.5-mo-old type III SMA mice (heterozygous for the A2G transgene, Het.), type III SMA mice (homozygous for the A2G transgene, Hom.), and normal mice (*Smn*$^{+/-}$) using the anti-SMN monoclonal antibody, MANSMA2. β-actin or β-tubulin serve as loading controls.

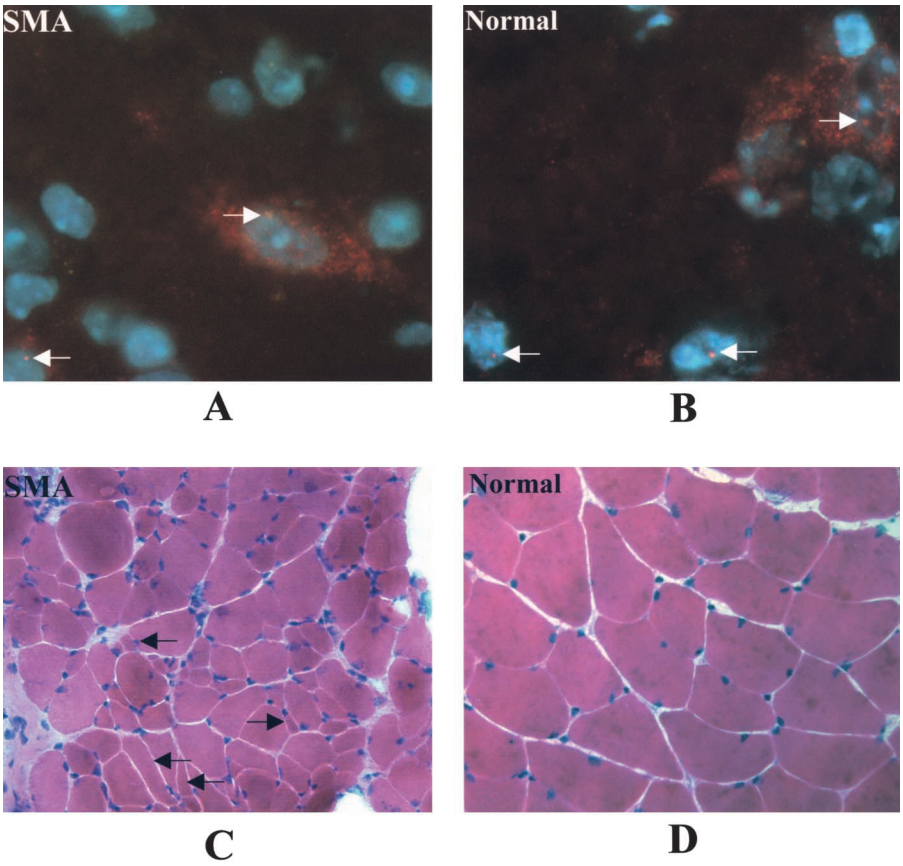

Figure 4. **Immunocytochemical staining of spinal cord, and hematoxylin and eosin staining of muscle.** Staining of SMN in spinal cord sections of (A) 1-mo-old *SMN A2G;SMN2;Smn*$^{-/-}$ type III SMA mouse and (B) an age-matched *Smn*$^{+/-}$control. Type III SMA mice express SMN in the motor neurons (arrows). However, nuclear gems in these animals are less intense and not as numerous as those seen in normal littermates. (600× magnification). Gastrocnemius from the same animals was sectioned and stained with hematoxylin and eosin. Numerous angulated and atrophied fibers (arrows) are evident in (C) type III SMA muscle as compared with (D) normal muscle (200× magnification).

Type III SMA mice exhibit muscle atrophy and partial restoration of gems in the spinal motor neurons

One of the most striking features of spinal muscular atrophy is the loss of the anterior horn cells (α motor neurons) of the spinal cord and a greatly reduced amount of SMN in these cells. We have previously shown that there is little or no staining of SMN in the motor neurons of type I SMA mice (Monani et al., 2000). To ascertain whether type III SMA mice express SMN in their spinal motor neurons, spinal cord sections from the lumbar and thoracic regions of 1-mo-old type III SMA mice, with a single copy of *SMN2* and heterozygous for the A2G transgene, and age-matched *Smn*$^{+/-}$ controls were immunocytochemically stained (Fig. 4, A and B). Based on the cytoplasmic staining and presence of gems in the spinal cord of diseased animals, it is clear that SMN is restored in motor neurons (Fig. 4 A). To quantitate the number of gems in the motor neurons of normal (n = 2) and type III SMA mice (n = 3), 10 different fields, under 600× magnification, from spinal cord sections of each mouse were selected and the gems counted. An average of 4.5 nuclear gems were counted per field (~60 nuclei) in type III SMA mice versus 9.8 nuclear gems in the age-matched controls. Thus it is clear that although SMN is easily detected in the spinal motor neurons of type III SMA mice, it is only a partial restoration.

A second characteristic feature of SMA is muscular atrophy due to denervation. We examined the gastrocnemius, quadriceps, and intercostal muscles of type III SMA mice from the above study to look for atrophy. Transverse sections of the gastrocnemius muscle showed numerous angulated and atrophic fibers (Fig. 4 C) compared with uniform-sized fibers in the age-matched controls (Fig. 4 D). This was less pronounced in the quadriceps and intercostal muscles of these animals (unpublished data), but is consistent with findings in some human type III SMA patients (Dubowitz, 1995).

Electrophysiological studies and evidence of axonal sprouting in type III SMA mice

To further characterize the muscle weakness in our type III SMA mice, EMG recordings were made on 4–6-mo-old *SMN2;Smn*$^{-/-}$ animals heterozygous for the mutant *SMN A2G* transgene. Recordings were made on resting muscle as it is difficult to obtain controlled, voluntary muscle contraction in mice. Normal muscle is electrically silent at rest and no spontaneous activity is detected after cessation of movement of the recording needle. In both of the type III (*1SMN A2G;SMN2;Smn*$^{-/-}$) animals we tested, we found abnormal spontaneous activity of single muscle fibers (fibrillation potentials) and of motor units (fasciculation potentials) accompanied occasionally by biphasic positive sharp waves (Fig. 5, A and B). These observations made on multiple pelvic (cranial tibial, vastus lateralis, and gastrocnemius; see Fig. S2, available online at http://www.jcb.org/cgi/content/full/jcb.200208079/DC1) and thoracic (suprascapular) muscles are a clear indication of denervation and provide a simple diagnosis of this process, as previously demonstrated in human patients (Dubowitz, 1995). We did not see abnormal electrical activity in age-matched type III SMA animals homozygous for the A2G transgene, indicating that increased levels of SMN from the A2G transgene correct this abnormality.

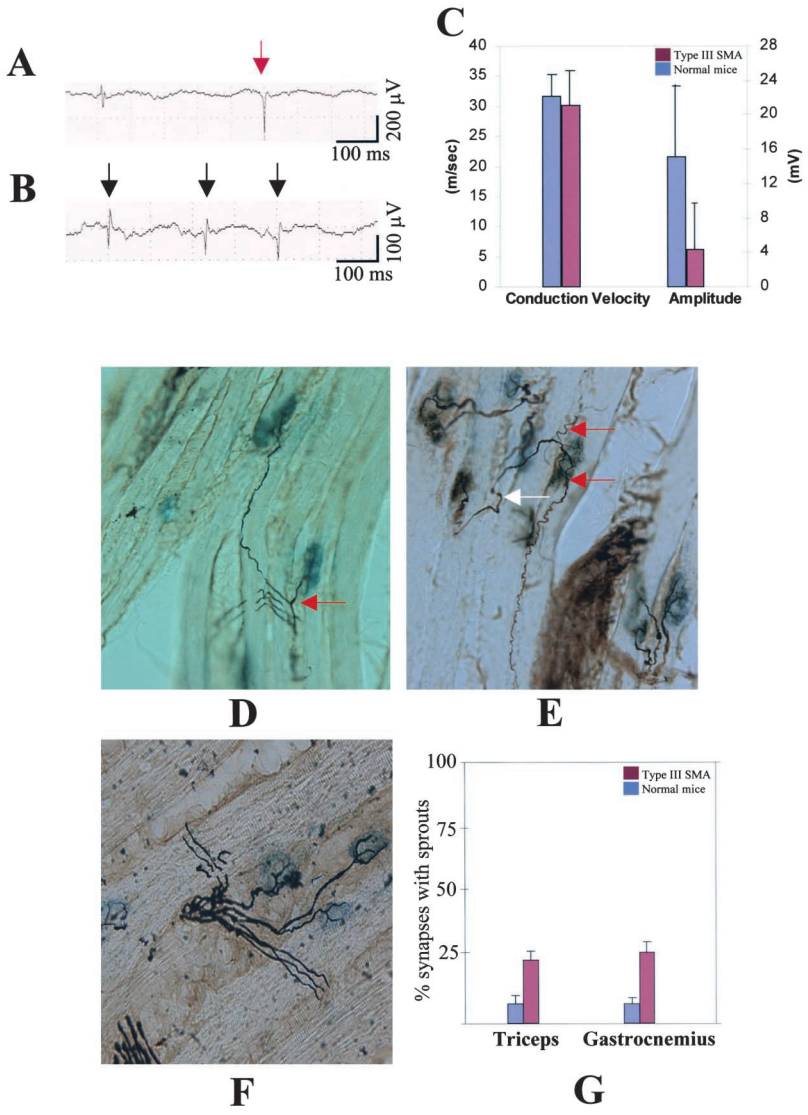

Figure 5. **Electromyography and axonal sprouting in mild SMN mice.** EMG recordings in (A) cranial tibial and (B) suprascapular muscle of 4-mo-old type III SMA mice. Spontaneous abnormal electrical activity was recorded in the form of fibrillation potentials (dark arrows) and occasional biphasic positive sharp waves (red arrow). (C) Quantification of MNCVs and the amplitudes of compound muscle action potentials in type III SMA mice and normal ($Smn^{+/+}$) littermates. At least four mice from each group were analyzed. Data are given as mean ± SD. Although the amplitude was reduced in SMA mice ($P < 0.05$, *t* test), the MNCVs did not significantly change. Axonal sprouting in the (D) gastrocnemius and (E) triceps of type III SMA mice is a further sign of denervation. The former is an example of nodal sprouting whereas the latter depicts terminal sprouts (red arrows). Arrow in white indicates main axonal branch. Motor axons are silver stained in black while neuromuscular junctions stain blue. Normal gastrocnemius (F) shows at least three different motor axons, each innervating a separate muscle fiber (running diagonally from lower left to upper right; magnification 400×). Graphical representation (G) of the extent of sprouting (terminal and nodal) in type III SMA mice and unaffected littermates. Data are given as mean ± SD.

This is consistent with data from some very mildly affected type III SMA patients (Hausmanowa-Petrusewicz and Karwanska, 1986). To assess the nature of the muscle weakness in mild SMA mice, we analyzed evoked compound action potentials and motor nerve conduction velocities (MNCVs) of the tibial nerve (Fig. 5 C). Although nerve conduction velocity tests on type III SMA (30.1 ± 5.6; $n = 4$) mice did not show a significant difference from those on age-matched controls (31.6 ± 3.3; $n = 4$), the amplitudes of the evoked muscle potentials were reduced (SMA, 4.3 ± 5.5, $n = 4$; normals, 15.07 ± 8.9, $n = 4$). These results indicate that demyelination of nerves is not a feature of SMA. Instead, it is likely that defects in neuronal axons contribute to SMA pathology in mildly affected mice.

To compensate for chronic denervation in motor neuron diseases, the surviving axons often sprout and reinnervate the denervated fibers. In rat soleus muscle, cross innervation by a foreign nerve at a site distant from the original end plate often preserves the old end plate. The original end plate may persist as long as 4 mo after the fiber has lost its nerve connection (Frank et al., 1976). We observed an increased number of neuromuscular junctions in the gastrocnemius of type III SMA mice (90; $n = 3$) compared with age-matched controls (51; $n = 3$). To investigate whether axonal sprouting might account for this, 50-μm sections of freshly frozen gastrocnemius, triceps, and intercostal muscle were dual stained for axons and acetylcholine-esterase activity. We show that sprouting does indeed occur both in type III SMA mice ($n = 3$) heterozygous for the A2G transgene as well as type III SMA mice homozygous for the A2G transgene (Fig. 5, D–G). Sprouts were nodal and were also seen to emerge from the neuromuscular junction (terminal sprouts). This was not observed in $Smn^{+/-}$ ($n = 2$) or eight-copy *SMN2;*$Smn^{-/-}$ mice (unpublished data) and is consistent with data from mild SMA patients (Vogt and Nix, 1997). To determine the extent of sprouting, synapses in the gastrocnemius and triceps muscles from mild SMA mice heterozygous for the A2G transgene ($n = 3$) and $Smn^{+/-}$ littermates ($n = 2$) were scored for the presence or absence of sprouts. Our data show that there is a significant increase in the number of sprouts in both gastrocnemius (SMA, 22 ± 4%; normal, 7 ± 2.5%) and triceps (SMA, 21 ± 3%; normal, 7.2 ± 3%) muscles of mild SMA mice (Fig. 5 G).

Table I. **Number of facial and spinal motor neurons in the brain stem and lumbar (L1–L6) spinal cord, respectively, of 3.5-mo-old *SMN2; Smn*$^{-/-}$ type III SMA mice heterozygous for the A2G transgene and age-matched controls**

Type of motor neurons	Type III SMA	Normal	Reduction
Facial nucleus	2,994 ± 94 (n = 4)	3,695 ± 171 (n = 2)	−19% ($P < 0.05$)
Spinal motor neurons	3,144 ± 201 (n = 4)	4,421 ± 76 (n = 2)	−29% ($P < 0.05$)

Motor neuron degeneration in type III SMA mice

To assess motor neuron degeneration in 3.5-mo-old *SMN2; Smn*$^{-/-}$ type III SMA mice heterozygous for the A2G transgene, transverse sections of the spinal lumbar region (unpublished data) and coronal sections of the facial nucleus (Fig. 6, A and B) were stained with cresyl echt violet and the morphology and numbers of the cells determined. The most obvious difference between the SMA mice and age-matched controls is a significant decrease in the numbers of motor neurons in the former. In the lumbar spinal cord, SMA mice have 29% fewer motor neurons than age-matched *Smn*$^{+/-}$ controls, while in the facial nucleus there is a ∼19% loss of motor neurons (Table I; Fig. 6, A and B). Previously, we showed a significant loss of motor neurons in the spinal cord and brain stem of 5-d-old severe SMA mice (Monani et al., 2000). To determine whether motor neuron loss occurs this early in type III SMA mice, 5-d-old *SMN2;Smn*$^{-/-}$ animals heterozygous for the A2G transgene were killed and motor neuron cell bodies in the facial nucleus counted. We found no evidence of motor neuron loss at this age in type III SMA mice (unpublished data). This is consistent with our previous finding that motor neuron loss is a late event in SMA. To further examine motor neuron degeneration, we also conducted ventral root counts on our type III SMA mice. Mice perfused with 4% paraformaldehyde, 1% glutaraldehyde were used to isolate the ventral roots from the L1–L5 lumbar spinal cord region. Semi-thin sections were cut, stained with toluidene blue (Fig. 6, C and D), and at least four different fields examined to quantitatively determine the number of motor axons in the roots of diseased mice and an age-matched control. Two striking differences were observed. First, type III SMA mice have fewer myelinated axons (Table II). The loss in motor axons correlates with the loss of motor neuron cell bodies in the spinal cord. Second, many of the remaining axons in the diseased mice are shriveled and exhibit signs of Wallerian degeneration (Fig. 6 D).

Discussion

Mice lacking murine *Smn* but carrying one to two copies of human *SMN2* provide a suitable animal model of type I spinal muscular atrophy (Hsieh-Li et al., 2000; Monani et al., 2000). In this study, we have introduced a transgene carrying a missense mutation in exon 1 of the *SMN* gene into the severe SMA genetic background. *SMN2;Smn*$^{-/-}$ mice that are heterozygous for the mutant transgene exhibit many of the clinical and pathological characteristics of type III (mild) SMA. These mice suffer from motor neuron degeneration and its associated effects. They include evidence of motor axon degeneration, loss and sprouting, muscle atrophy, and abnormal EMG patterns. Other obvious clinical features of SMA in our mice include muscle weakness, reduced activity, and a decreased life span. In keeping with numerous previous studies showing a tight correlation between levels of *SMN2* copy number/SMN protein and disease severity, *SMN2; Smn*$^{-/-}$ mice homozygous for the mutant transgene exhibit a very mild disease phenotype. Indeed, there are few overt signs of muscle weakness in 6-mo-old animals and a relatively prolonged lifespan (≥15 mo) compared with heterozygous *SMN A2G* transgenic mice. We have previously shown that type I SMA mice lose 35–40% of their motor neurons by the time they die, while Jablonka et al. (2000) showed up to 50% spinal motor neuron loss in 12-mo-old *Smn*$^{+/-}$ animals. Yet type I SMA mice rarely live beyond 6 d of age, whereas *Smn*$^{+/-}$ animals live completely normal lives and exhibit no clinical signs of SMA. The implications are, first, that a 50% motor neuron loss is completely compatible with life and, second, that the surviving motor neurons in type I SMA mice are too sick to function normally thus resulting in early death. Motor neuron loss in type III SMA mice occurs significantly earlier than in *Smn*$^{+/-}$ heterozygotes but not as early as in type I SMA mice. The widely varying phenotypes but similar numbers of motor neurons lost in severe, mild, and *Smn*$^{+/-}$ mice imply that the timing of cell loss, rather than the actual numbers lost, is important. Disease symptoms in type III SMA mice, as evidenced by muscle weakness, occur as early as 1 mo of age. If, as we suspect, onset of the disease correlates with motor neuron dysfunction, we would expect to see electrophysiological abnormalities at this age. Interestingly, recent similar studies involving motor unit number estimation (MUNE) in pre- and post-symptomatic human patients revealed that a large number of motor neurons are present before the onset of the phenotype and that there is a rapid decline in the numbers of motor units with disease progression (Bromberg and Swoboda, 2002). This is similar to studies involving morphometric counts in severe SMA mice, which show a correlation between motor neuron loss and onset of disease symptoms. As EMG studies can be performed on mild SMA mice, it will be possible to correlate motor neuron counts with MUNE/EMG studies in order to determine if neuronal loss in SMA occurs as a dying back process, as has been found in another mouse model of motor neuron disease (Holtmann et al., 1999).

It is intriguing to consider how the A2G mutation on an *SMN2;Smn*$^{-/-}$ background results in a mild SMA phenotype. The mutation is the most 5′ one reported so far. It is neither in the oligomerization domain in exon 6 nor in exon

Table II. **Number of motor axons in the lumbar ventral roots of type III SMA mice and normals**

Age (mo)	Type III SMA	Normal	Reduction
5	599 ± 61 (n = 4)	801 ± 90 (n = 5)	−25% ($P < 0.05$)

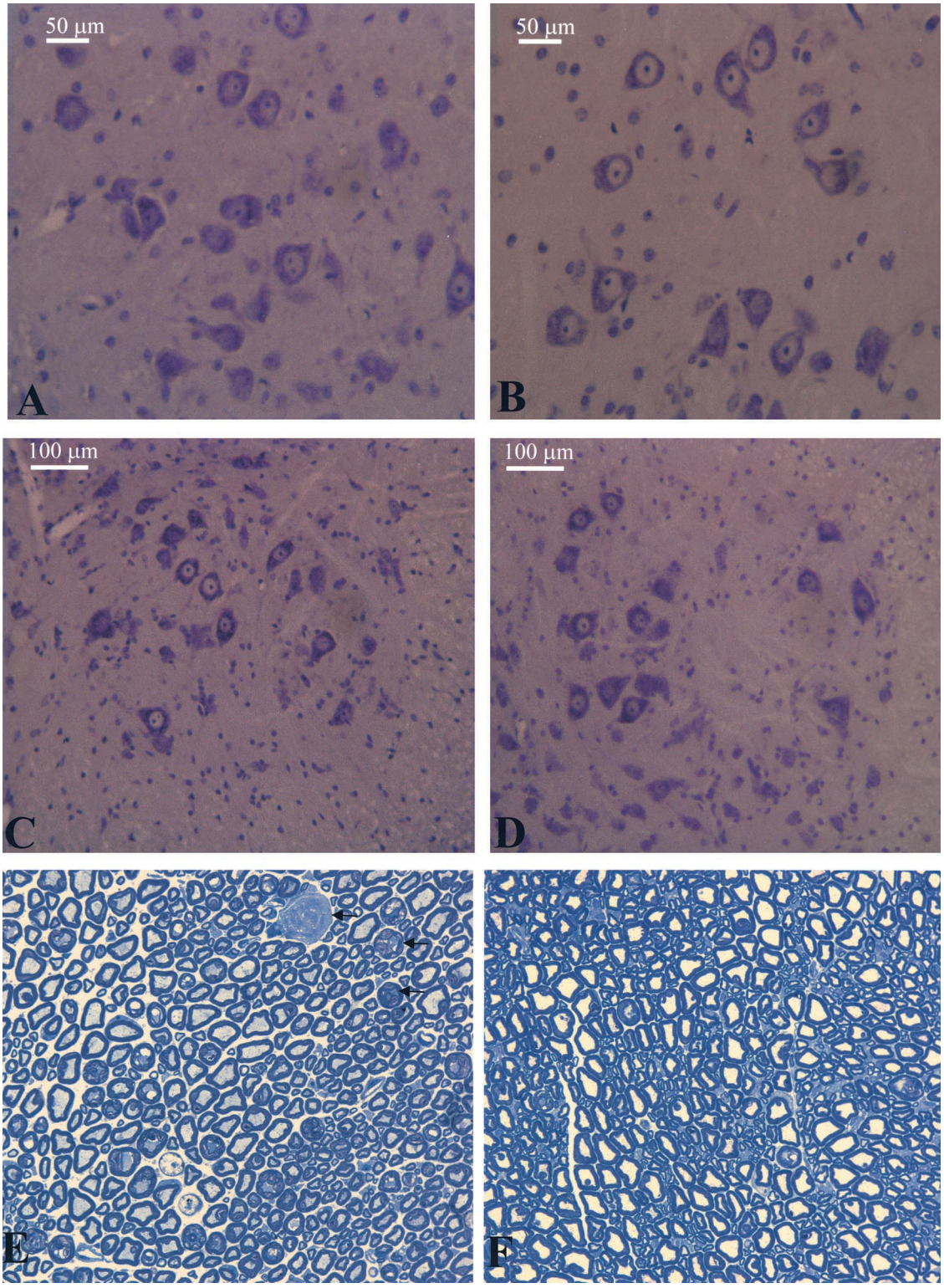

Figure 6. **Motor neuron cell bodies and ventral roots in mild SMA mice.** Motor neuron degeneration in the (A) facial nucleus and (C) lumbar spinal cord of a 3.5-mo-old type III SMA mouse showing fewer cells with intact nuclei compared with the normal $Smn^{+/-}$ control in B and D, respectively. An examination of the motor axons in the ventral roots of (E) type III SMA mice by toluidine blue staining shows a myelin ovoid and numerous axons undergoing Wallerian degeneration (arrows). F represents an age-matched normal control (magnification 600×).

2b. It is not in the Sm protein binding domain nor does it affect SIP-1 binding (unpublished data). Yet, we have shown that the A2G mutation does disrupt self-association and affects SmN binding presumably by disrupting the formation of SMN oligomers. A to G mutations have been shown to profoundly affect α-helices (Lyu et al., 1990; Chakrabartty et al., 1991). It is not unlikely that the mutation disrupts the three-dimensional structure of the protein enough to affect

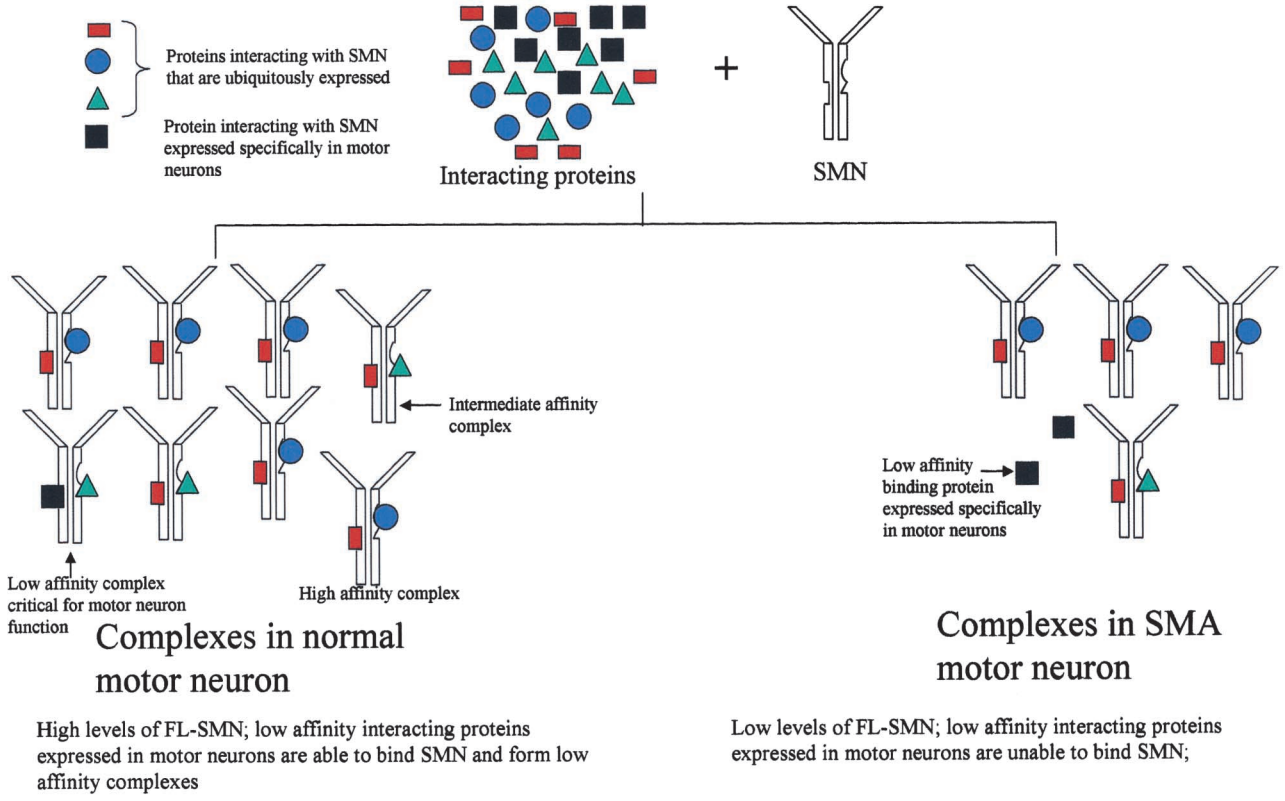

Figure 7. **A molecular model of SMA that may explain the motor neuron specificity of the disease.** A protein with a low affinity for SMN expressed selectively in the motor neurons would be unable to bind and form a functional complex in these cells in an SMA patient. This would result in degeneration and loss of motor neurons but not other tissues.

the oligomerization domains in exon 2b and/or exon 6 as well as the Sm binding domain. Although the A2G protein retains some level of self-association activity, it is possible this deficiency results in that mutant's inability to form higher order complexes necessary for SMN function and interactions with protein partners. This could explain why SMN A2G does not rescue $Smn^{-/-}$ embryonic lethality. If, however, full-length SMN serves as a scaffold, then low levels of the protein might promote the formation of higher order FL-SMN:SMN A2G oligomers with an enhanced ability to bind other interacting proteins such as SmN. Our data show that SMN A2G binds with a higher affinity to FL-SMN than does Δ7 SMN. FL-SMN:SMN A2G complexes would therefore be more stable than FL-SMN:Δ7 SMN ones. Furthermore, it has been shown that protein levels in patients with missense mutations correlate with the disease phenotype (Lefebvre et al., 1997). These data and our observations lead us to a plausible molecular model of SMA (Fig. 7) in which SMN forms a number of complexes with different partners. These partners compete for the same sites on SMN, binding being determined by their relative affinities for SMN. In the presence of low levels of full-length SMN, low affinity binding partners are out-competed by high affinity proteins. It is possible that the low affinity binding partners are selectively found in motor neurons and are unable to form functional complexes in SMA patients due to the low SMN levels. Loss or disruption of the low affinity complex in motor neurons would result in the degeneration of these, but not other, tissues. Our model is consistent with the observation of increased SMN levels and a mild phenotype in mice carrying the A2G missense mutation on a severe SMA genetic background.

Despite recent advances in elucidating the functions of SMN, including studies implicating SMN to be important in neural growth cones and in RNA editing/transport in motor axons (Fan and Simard, 2002; Rossol et al., 2002), the selective loss of α motor neurons in SMA remains far from clear. The functions attributed to SMN would seem to be important in all cells, yet it is the motor neuron that is most profoundly affected. The presence of a low affinity SMN interacting partner in these but not other cells may explain the specificity of the disease. A majority of the mutations in SMA affect either oligomerization, binding of one of SMN's interacting partners, or both. This has been assessed either in vitro or in cell culture but not in motor neurons. It is unclear whether the same function(s) is disrupted in these cells in a diseased animal. Our type III SMA mice may allow us to address this by providing us with the ability to create motor neuron cell lines and study the effect of the A2G missense mutation on the SMN macromolecular complex. What is clear is that the A2G missense mutation is unable to rescue embryonic lethality in $Smn^{-/-}$ mice. Because this is a mild mutation, we would expect severe missense mutations to have the same effect. This is in contrast to a study by Wang and Dreyfuss (2001) in which they report the ability of a number of missense mutations to rescue lethality in a chicken cell line. Two ways of explaining our discordant results are, first, leaky expression of very low levels of full-

length SMN in the chicken cell line, and, second, a critical requirement for intact SMN during development in a whole animal, but not in a cell line, which is disrupted in its absence, leading to embryonic lethality. A number of groups have reported compounds capable of increasing SMN from *SMN2*. It will be important to assess these in an appropriate animal model of SMA. The mild SMA mouse we have generated here has certain distinct advantages over previously reported animal models. It has a clear and consistent SMA phenotype but is more robust than severe SMA mice and therefore amenable to drug administration protocols. We have shown that denervation in mild SMA mice may be measured electrophysiologically. Additionally, the abnormal EMGs indicative of denervation correlate with SMN protein levels. Standard EMG analysis could be complemented with MUNE studies, which would serve to further refine ways of measuring the outcome of any drug treatment studies. It is therefore clear that our mice are an important tool in (a) ensuring the safety and efficacy of drugs/molecules that we and others are currently isolating in high-throughput screens and (2) the evaluation of gene therapy procedures for SMA.

Materials and methods

Generation of transgenic mice and breeding strategy

A forward primer, 5′-GCAGGATCCTATGGGGATGAGCAGCGG-3′, in SMN exon 1 containing an engineered BamHI site and the C to G transition, which results in the A2G mutation, and a reverse primer in exon 8, 5′-CCGAATTCAGTACAATGAACAGCCATGTCCACC-3′, containing an EcoRI site were used to amplify SMN by RT-PCR. The ~1.5-kb product was digested with BamHI and EcoRI and cloned into the pcDNA3 (Invitrogen) vector. Separately, a ~3.4-kb KpnI–SacII SMN promoter fragment was cloned into the pEGFP (CLONTECH Laboratories, Inc.) vector and then excised out using KpnI and BamHI. This fragment was directionally ligated to the SMN cDNA in pcDNA3. The 4.9-kb promoter–SMN transgene was then excised with KpnI and BamHI and injected into fertilized FVB mouse oocytes. Potential founders were screened by Southern analysis using an exon 6–8 SMN cDNA probe or by PCR using the following primers: 4.5F, 5′-ACTGGGACCAGGAAAGCCGGT-3′, and 6R, 5′-GCCAGTATGATAGCCACTCATG-3′. Founders were bred to *SMN2;Smn*$^{+/-}$ mice we have previously generated. *SMN A2G;SMN2;Smn*$^{+/-}$ animals were then either interbred or backcrossed with *SMN2;Smn*$^{+/-}$ mice, resulting in *SMN A2G;SMN2;Smn*$^{-/-}$ animals.

In vitro binding assays

SMN A2G, FL-SMN, and Δ7 SMN cDNAs were subcloned into the vector pGEX-3X (Amersham Biosciences). GST fusion proteins were prepared and purified using glutathione-linked agarose beads as previously described (Lorson et al., 1998). To prepare ^{35}S-labeled SMN proteins, the T7 transcription/translation (TnT) rabbit reticulocyte lysate system (Promega) was used. The protocol was essentially the same as that described by Lorson et al. (1998) except that densitometry was performed using a Phosphorimager (Molecular Dynamics, Inc.)

RT-PCR, Southern, and Western analysis

To determine the expression of the mutant A2G transgene, *Smn*$^{+/+}$ carrying the transgene but no *SMN2* were killed by cervical dislocation and polyA$^+$ RNA was isolated using the QuickPrep Micro mRNA purification kit (Amersham Biosciences) according to the manufacturer's recommendations. After treating the RNA with DNase I to get rid of contaminating genomic DNA, ~100 ng was reverse transcribed and amplified using the following human *SMN*-specific primers in exons 1 and 4, respectively: Ex1F, 5′-GCGGCGGCAGTGGTGGCGGC-3′, and Ex4R, 5′-TGGAGCAGATTTGGGCTTGA-3′. Native murine *Smn* and the knockout allele were followed by Southern blot analysis after Bam HI digestion of tail DNA using a probe in *Smn* intron 1. The probe was radioactively labeled and hybridized to the filter containing the DNA according to standard methods. The filter was washed at high stringency and then exposed to Hyperfilm MP (Amersham Biosciences) with an intensifying screen. Copy number of the SMN A2G transgene was determined by Southern blot analysis of DNA from *SMN A2G;Smn*$^{+/+}$ animals. An SMN exon 6–8 cDNA fragment and a murine *Smn* intron 1 probe of approximately equal length and GC content were radioactively labeled and simultaneously hybridized to the blot. The blot was washed and exposed to film as described above. Intensities of bands corresponding to the transgene were then determined using a Shimadzu 9000 CS scanner. Copy number was determined by comparing the intensities of these bands to those of the single-copy murine *Smn* gene in each animal. For Western blot analysis, 100 mg of tissue from 5-d-old mice was dissolved in blending buffer (10% SDS, 62.5 mM Tris, pH 6.8, 5 mM EDTA). 25–50 μg of protein was mixed with an equal volume of sample buffer (62.5 mM Tris, pH 6.8, 10% glycerol, 10% 2 ME, 0.4 mg bromophenol blue) and electrophoresed on a 12.5% polyacrylamide gel. Samples were transferred to Immobilon P (Millipore) as previously described (Coovert et al., 1997). The blot was blocked in 5% milk powder, 0.5% BSA in TBS-Tween for 2 h, and then incubated for 1 h with anti-SMN primary antibody (MANSMA2). Bound primary antibody was detected by HRP-conjugated secondary antibody followed by chemiluminescence (Amersham Biosciences). The blots were then stripped and reprobed with a β-actin antibody to control for loading amounts.

Histology and immunocytochemistry

For hematoxylin-eosin stains and spinal cord immunocytochemistry, adult type III SMA mice and normal controls were killed by CO_2 gas, transcardially perfused briefly with cold 1× PBS, and the muscle and spinal cord tissue dissected out, mounted on wooden blocks, and flash frozen in liquid nitrogen–cooled isopentane. 10–12-μm thick transverse muscle sections were cut, mounted on Superfrost (Fisher Scientific) slides, and then air dried before processing. Sections were fixed in 100% alcohol (30 s), rinsed in tap water, and stained in hematoxylin (Sigma-Aldrich) for 30 s followed by a second rinse in tap water. They were then stained in eosin (Sigma-Aldrich) for 20 s, rinsed in tap water, dehydrated in alcohol, and cleared in xylene before mounting in Permount (Sigma-Aldrich) for light microscopy. Immunocytochemistry on spinal cord sections was essentially performed as described previously (Monani et al., 2000). For motor neuron studies and ventral root counts, mice were transcardially perfused with 1× PBS followed by 4% paraformaldehyde, 1% glutaraldehyde. Ventral roots, lumbar spinal cord, and the brain stem were post-fixed for 24 h in the same solution. The brain stem and spinal cord were then embedded in paraffin according to conventional procedures. Serial sections (6 μm) prepared with a rotary microtome (American Optical Instruments) were mounted on glass slides and Nissl's stained as previously described (Sendtner et al., 1990). Ventral roots were post-fixed in 1% osmium tetroxide (1 h), rinsed in 0.1 M phosphate buffer (pH 7.3), and then dehydrated. They were then embedded in Spurr resin and 0.5-μm sections were cut on a Reichert Ultracut E microtome. Sections were stained with toluidine blue and visualized by light microscopy.

To look for axonal sprouting in type III SMA mice, animals were killed by cervical dislocation and the intercostals, gastrocnemius, and triceps muscles were dissected out. Muscle tissue was immersed in 3% disodium EDTA for 20 s, mounted on wooden blocks, and flash frozen in liquid nitrogen–cooled isopentane. 50-μm thick longitudanal sections were cut in a cryostat and placed on Superfrost (Fisher Scientific) slides. A drop of 3% disodium EDTA was immediately placed on the sections to prevent muscle contracture and the sections were allowed to air dry. Cholinesterase and axonal staining were performed as described previously (Pestronk and Drachman, 1978), except that sections were stained in a 10% rather than 20% silver nitrate solution for 10 min. We found this reduces the extent of muscle fiber shrinkage and separation and better preserves the integrity of intramuscular nerves. To determine the extent of sprouting, synapses in ten 50-μm thick sections from the gastrocnemius (medial and lateral parts) and triceps were examined. The 500-μm portion included the middle of the muscle and sections on either side. Synapses were systematically scored for those with or without sprouts. Terminal and nodal sprouts were combined and expressed as a percentage of the total readable synapses. Approximately 400 synapses in each muscle were scored.

Electrophysiological studies

4–6-mo-old mice were anesthetized with an intraperitoneal injection of a mixture of ketamine (60 mg/kg) and xylazine (3.5 mg/kg). They were maintained at 34°C under anesthesia using isofluorine. For EMG testing, a monopolar needle (26 gauge; Electrode store) was used. Intramuscular potentials were recorded on an EMG instrument (model Neuropack Four mini [MEB-5304K]; Nihon Kohden Corp.). Muscle EMG testing was grouped into the following sites: proximal thoracic limb muscles, proximal pelvic limb muscles, distal thoracic limb muscles, distal pelvic limb mus-

cles, cervical epaxial muscles, and remaining epaxial muscles. The minimum criteria used to define the presence of spontaneous activity was the persistence of an abnormal waveform (>3 s) after complete cessation of needle movement that was reproducible with redirection of the EMG needle. MNCV recordings of the tibial nerve were performed with an Evoked Potential Measuring System. Subdermal stimulating electrodes (10-mm platinum safelead electrodes, model F-E2; Grass Instruments) were placed at the sciatic notch (proximal stimulation site) and the head of the fibula (distal stimulation site) for the sciatic nerve (upper tibial) evaluation. The distal portion of the tibial nerve was evaluated by placing subdermal stimulating electrodes at the head of the fibula (proximal stimulation site) and the ankle (distal stimulation site). Percutaneous intramuscular recording and reference electrodes (26 gauge, 40 × 0.45-mm monopolar needles; Dantec Neurosupplies) were placed on the extensor digitorum brevis muscle of the lateral toe. A ground subcutaneous electrode was placed over the ankle. Stimulation was performed with a single square wave pulse of 0.2-ms duration at 1 Hz with a current of 10–15 mA. Reading parameters for the M wave are an analysis time of 10 ms, sensitivity of 10 mV, and band filter of 50–3,000 Hz. Motor nerve conduction was determined by the formula Velocity (ms) = distance/time. Distance was measured using a flexible tape between the cathodes of each stimulation site.

Online supplemental material

The supplemental material (Figs. S1 and S2) is available online at http://www.jcb.org/cgi/content/full/jcb.200208079/DC1. Fig. S1 shows survival curves for mild SMA mice, and Fig. S2 shows EMG results in the muscles indicated.

We thank Dr. J. Rafael for critically reading our manuscript and Dr. G. Bishop for technical help.

This study was supported by Families of SMA (FSMA), the Madison Fund, National Institutes of Health grants NS 38650 to A.H.M. Burghes and NS 40275 to E.J. Androphy. M. Sendtner is supported by a grant from the Deutsche Forschungsgemeinschaft (To61/8-4). U. Monani and C. Andreassi are the recipients of a development grant from the Muscular Dystrophy Association of America and a postdoctoral fellowship from FSMA, respectively.

Submitted: 13 August 2002
Revised: 27 November 2002
Accepted: 2 December 2002

References

Andreassi, C., J. Jarecki, J. Zhou, D.D. Coovert, U.R. Monani, X. Chen, M. Whitney, B. Pollock, M. Zhang, E. Androphy, and A.H.M. Burghes. 2001. Aclarubicin treatment restores SMN levels to cells derived from type I spinal muscular atrophy patients. *Hum. Mol. Genet.* 10:2841–2849.

Baron-Delage, S., A. Abadie, A. Echaniz-Laguna, J. Melki, and L. Beretta. 2000. Interferons and IRF-1 induce expression of the survival motor neuron (SMN) genes. *Mol. Med.* 6:957–968.

Bromberg, M.B., and K.J. Swoboda. 2002. Motor unit number estimation in infants and children with spinal muscular atrophy. *Muscle Nerve.* 25:445–447.

Buhler, D., V. Raker, R. Luhrmann, and U. Fischer. 1999. Essential role for the tudor domain of SMN in spliceosomal U snRNP assembly: implications for spinal muscular atrophy. *Hum. Mol. Genet.* 8:2351–2357.

Bussaglia, E., O. Clermont, E. Tizzano, S. Lefebvre, L. Burglen, C. Cruaud, J. Urtizberrea, J. Colomer, A. Munnich, and M. Baiget. 1995. A frame-shift deletion in the survival motor neuron gene in Spanish spinal muscular atrophy patients. *Nat. Genet.* 11:335–337.

Campbell, L., A. Potter, J. Ignatius, V. Dubowitz, and K.E. Davies. 1997. Genomic variation and gene conversion in spinal muscular atrophy: implications for disease process and clinical phenotype. *Am. J. Hum. Genet.* 61:40–50.

Campbell, L., K.M. Hunter, P. Mohaghegh, J.M. Tinsley, M.A. Brasch, and K.E. Davies. 2000. Direct interaction of Smn with dp103, a putative RNA helicase: a role for Smn in transcription regulation. *Hum. Mol. Genet.* 9:1093–1100.

Chakrabartty, A., J.A. Schellman, and R.L. Baldwin. 1991. Large differences in the helix propensities of alanine and glycine. *Nature.* 351:586–588.

Chang, J.G., H.M. Hsieh-Li, Y.J. Jong, N.M. Wang, C.H. Tsai, and H. Li. 2001. Treatment of spinal muscular atrophy by sodium butyrate. *Proc. Natl. Acad. Sci. USA.* 98:9808–9813.

Charroux, B., L. Pellizoni, R.A. Perkinson, A. Shevchenko, M. Mann, and G. Dreyfuss. 1999. Gemin 3: a novel DEAD box protein that interacts with SMN, the spinal muscular atrophy gene product, and is a component of gems. *J. Cell Biol.* 147:1181–1193.

Coovert, D., T.T. Le, P. McAndrew, J. Strasswimmer, T.O. Crawford, J.R. Mendell, S. Coulson, E.J. Androphy, T.W. Prior, and A.H.M. Burghes. 1997. The survival motor neuron protein in spinal muscular atrophy. *Hum. Mol. Genet.* 6:1205–1214.

Crawford, T.O., and C.A. Pardo. 1996. The neurobiology of childhood spinal muscular atrophy. *Neurobiol. Dis.* 3:97–110.

Dubowitz, V. 1995. Muscle Disorders in Childhood. Third Edition. Saunders, Philadelphia. 354 pp.

Fan, L., and L. Simard. 2002. Survival motor neuron (SMN) protein: role in neurite outgrowth and neuromuscular maturation during neuronal differentiation and development. *Hum. Mol. Genet.* 11:1605–1614.

Fischer, U., Q. Liu, and G. Dreyfuss. 1997. The SMN-SIP1 complex has an essential role in spliceosomal snRNP biogenesis. *Cell.* 90:1023–1029.

Frank, E., K. Gautvik, and H. Sommerschild. 1976. Persistence of junctional acetylcholine receptors following denervation. *Cold Spring Harb. Symp. Quant. Biol.* 40:275–281.

Gangwani, L., M. Mikrut, S. Theroux, M. Sharma, and R.J. Davis. 2001. Spinal muscular atrophy disrupts the interaction of ZPR1 with the survival motor neurons protein. *Nat. Cell Biol.* 3:376–383.

Hahnen, E., J. Schonling, S. Rudnik-Schoneborn, H. Raschke, K. Zerres, and B. Wirth. 1997. Missense mutations in exon 6 of the survival motor neuron gene in patients with spinal muscular atrophy (SMA). *Hum. Mol. Genet.* 6:821–825.

Hausmanowa-Petrusewicz, I., and A. Karwanska. 1986. Electromyographic findings in different forms of infantile and juvenile proximal spinal muscular atrophy. *Muscle Nerve.* 9:37–46.

Holtmann, B., J. Zielasek, K.V. Toyka, and M. Sendtner. 1999. Comparative analysis of motoneruon loss and functional deficits in PMN mice: implications for human motoneuron disease. *J. Neurol. Sci.* 169:140–147.

Hsieh-Li, H., J.-G. Chang, Y.-J. Jong, M.-H. Wu, N. Wang, C.H. Tsai, and H. Li. 2000. A mouse model for spinal muscular atrophy. *Nat. Genet.* 24:66–70.

Jablonka, S., B. Schrank, M. Kralewski, W. Rossol, and M. Sendtner. 2000. Reduced survival motor neuron (*Smn*) gene dose in mice leads to motor neuron degeneration: an animal model for spinal muscular atrophy type III. *Hum. Mol. Genet.* 9:341–346.

Jones, K.W., K. Gorzynski, C.M. Hales, U. Fischer, F. Badbanchi, R.M. Terns, and M.P. Terns. 2001. Direct interaction of the spinal muscular atrophy disease protein SMN with the small nucleolar RNA-associated protein fibrillarin. *J. Biol. Chem.* 276:38645–38651.

Lefebvre, S., L. Burglen, S. Reboullet, O. Clermont, P. Burlet, L. Viollet, B. Benichou, C. Cruaud, P. Millasseau, and M. Zeviani. 1995. Identification and characterization of spinal muscular atrophy-determining gene. *Cell.* 80:155–165.

Lefebvre, S., P. Burlet, Q. Liu, S. Bertrandy, O. Clermont, A. Munnich, G. Dreyfuss, and J. Melki. 1997. Correlation between severity and SMN protein level in spinal muscular atrophy. *Nat. Genet.* 16:265–269.

Liu, Q., and G. Dreyfuss. 1996. A novel nuclear structure containing the survival motor neurons protein. *EMBO J.* 15:3555–3564.

Liu, Q., U. Fischer, F. Wang, and G. Dreyfuss. 1997. The spinal muscular atrophy disease gene product, SMN, and its associated protein, SIP-1, are in a complex with spliceosomal snRNP proteins. *Cell.* 90:1013–1022.

Lorson, C.L., and E.J. Androphy. 2000. An exonic enhancer is required for inclusion of an essential exon in the SMA determining gene SMN. *Hum. Mol. Genet.* 9:259–265.

Lorson, C.L., J. Strasswimmer, J.M. Yao, J.D. Baleja, E. Hahnen, B. Wirth, T.T. Le, A.H.M. Burghes, and E.J. Androphy. 1998. SMN oligomerization defect correlates with spinal muscular atrophy. *Nat. Genet.* 19:63–66.

Lorson, C.L., E.J. Hahnen, E. Androphy, and B. Wirth. 1999. A single nucleotide in the SMN gene regulates splicing and is responsible for spinal muscular atrophy. *Proc. Natl. Acad. Sci. USA.* 96:6307–6311.

Lyu, P.C., M.I. Liff, L.A. Marky, and N.R. Kallenbach. 1990. Side chain contributions to the stability of α-helical structure in peptides. *Science.* 250:669–673.

McAndrew, P.E., D.W. Parsons, L.R. Simard, C. Rochette, P. Ray, J.R. Mendell, T.W. Prior, and A.H.M. Burghes. 1997. Identification of proximal spinal muscular atrophy carriers and patients by analysis of *SMNT* and *SMNC* copy number. *Am. J. Hum. Genet.* 60:1411–1422.

Melki, J. 1997. Spinal muscular atrophy. *Curr. Opin. Neurol.* 10:381–385.

Monani, U.R., C.L. Lorson, D.W. Parsons, T.W. Prior, E.J. Androphy, A.H.M. Burghes, and J.D. McPherson. 1999a. A single nucleotide difference that alters splicing patterns distinguishes the SMA gene SMN1 from the copy gene SMN2. *Hum. Mol. Genet.* 8:1177–1183.

Monani, U.R., J.D. McPherson, and A.H.M. Burghes. 1999b. Promoter analysis

of the human centromeric and telomeric survival motor neuron genes (SMN^C and SMN^T). *Biochim. Biophys. Acta.* 1445:330–336.

Monani, U.R., M. Sendtner, D.D. Coovert, D.W. Parsons, C. Andreassi, T.T. Le, S. Jablonka, B. Schrank, W. Rossol, T.W. Prior, et al. 2000. The human centromeric survival motor neuron gene (SMN2) rescues embryonic lethality in $Smn^{-/-}$ mice and results in a mouse with spinal muscular atrophy. *Hum. Mol. Genet.* 9:333–339.

Munsat, T.L., and K.E. Davies. 1992. Meeting report: International SMA Consortium meeting. *Neuromusc. Disord.* 2:423–428.

Parsons, D.W., P. McAndrew, U.R. Monani, J.R. Mendell, A.H.M. Burghes, and T.W. Prior. 1996. An 11bp duplication in exon 6 of the SMN gene produces a type I spinal muscular atrophy phenotype: further evidence for SMN as the SMA-determining gene. *Hum. Mol. Genet.* 5:1727–1732.

Parsons, D.W., P.E. McAndrew, S.T. Iannoccone, J.R. Mendell, A.H.M. Burghes, and T.W. Prior. 1998. Intragenic telSMN mutations: frequency, distribution, evidence of a founder effect, and modification of the spinal muscular atrophy phenotype by cenSMN copy number. *Am. J. Hum. Genet.* 63: 1712–1723.

Pellizzoni, L., N. Kataoka, B. Charroux, and G. Dreyfuss. 1998. A novel function for SMN, the spinal muscular atrophy disease gene product, in pre-mRNA splicing. *Cell.* 95:615–624.

Pellizzoni, L., J. Baccon, B. Charroux, and G. Dreyfuss. 2001a. The survival of motor neurons (SMN) protein interacts with the snoRNP proteins fibrillarin and GAR1. *Curr. Biol.* 11:1079–1088.

Pellizzoni, L., B. Charroux, J. Rappsilber, M. Mann, and G. Dreyfuss. 2001b. A functional interaction between the survival motor neuron complex and RNA polymerase II. *J. Cell Biol.* 152:75–85.

Pestronk, A., and D.B. Drachman. 1978. A new stain for quantitative measurement of sprouting at neuromuscular junctions. *Muscle Nerve.* 1:70–74.

Roberts, D.F., J. Chavez, and S.D.M. Court. 1970. The genetic component in child mortality. *Arch. Dis. Child.* 45:33–38.

Rossol, W., A.-K. Kroning, U.-M. Ohndorf, C. Steegborn, S. Jablonka, and M. Sendtner. 2002. Specific interaction of Smn, the spinal muscular atrophy determining gene product, with hnRNP-R and gry-rbp/hnRNP-Q: a role for Smn in RNA processing in motor axons? *Hum. Mol. Genet.* 11:93–105.

Schrank, B., R. Gotz, J.M. Gunnerson, J.M. Ure, K. Toyka, A. Smith, and M. Sendtner. 1997. Inactivation of the survival motor neuron gene, a candidate gene for human spinal muscular atrophy, leads to massive cell death in early mouse embryos. *Proc. Natl. Acad. Sci. USA.* 94:9920–9925.

Sendtner, M., G.W. Kreutzberg, and H.J. Thoenen. 1990. Ciliary neurotrophic factor prevents the degeneration of motor neurons after axotomy. *Nature.* 345:440–441.

Strasswimmer, J., C.L. Lorson, D.E. Breiding, J.J. Chen, T. Le, A.H.M. Burghes, and E.J. Androphy. 1999. Identification of survival motor neuron as a transcriptional activator-binding protein. *Hum. Mol. Genet.* 8:1219–1226.

Talbot, K., C.P. Ponting, A.M. Theodosiou, N. Rodrigues, R. Surtees, R. Mountford, and K.E. Davies. 1997. Missense mutation clustering in the survival motor neuron gene: a role for a conserved tyrosine and glycine rich region of the protein in RNA metabolism? *Hum. Mol. Genet.* 6:497–501.

Terns, M.P., and R.M. Terns. 2001. Macromolecular complexes: SMN–the master assembler. *Curr. Biol.* 11:R862–R864.

Vogt, T., and W.A. Nix. 1997. Functional properties of motor units in motor neuron diseases and neuropathies. *Electroencephalogr. Clin. Neurophysiol.* 105: 328–332.

Wang, J., and G. Dreyfuss. 2001. Characterization of functional domains of the SMN protein in vivo. *J. Biol. Chem.* 276:45387–45393.

Young, P.J., N.T. Man, C.L. Lorson, T.T. Le, E.J. Androphy, A.H.M. Burghes, and G.E. Morris. 2000. The exon 2b region of the spinal muscular atrophy protein, SMN, is involved in self-association and SIP1 binding. *Hum. Mol. Genet.* 9:2869–2877.

Young, P.J., T.T. Le, M. Dunckley, T.M. Nguyen, A.H.M. Burghes, and G.E. Morris. 2001. Nuclear gems and Cajal (coiled) bodies in fetal tissues: nucleolar distribution of the spinal muscular atrophy protein, SMN. *Exp. Cell Res.* 265:252–261.

Zhang, M.L., C.L. Lorson, E.J. Androphy, and J. Zhou. 2001. An in vivo reporter system for measuring increased inclusion of exon 7 in SMN2 mRNA: potential therapy of SMA. *Gene Ther.* 8:1532–1538.